



Analysis and calibration of the VLP-16 for automotive applications

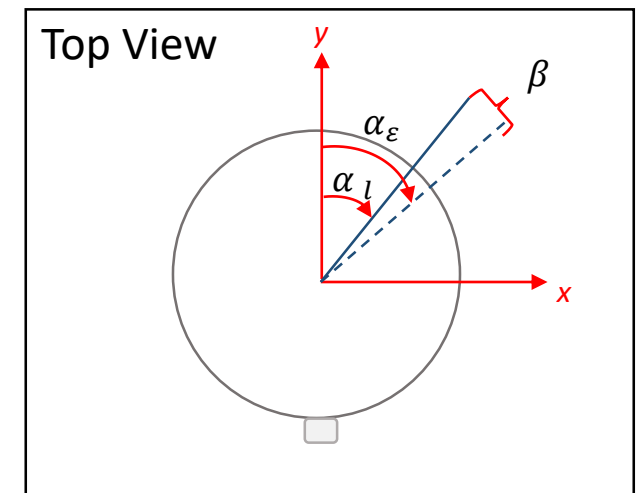
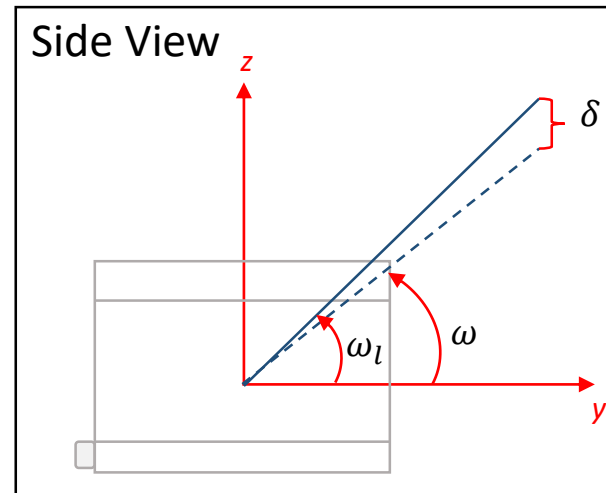
Daniela Sánchez
ION GNSS+ 2019

Outline

- **Introduction**
- **Previous work**
- **Calibration setup**
- **Data processing**
- **Results**
- **Conclusions**

Introduction

- Many terrestrial laser scanner applications, and specifically precise localization for autonomous driving using LiDAR, demand accurate and precise measurements.
- Systematic errors can be found in the instrumentation due to imperfections during the manufacture and assembly of the sensor.
- Parameters that can be modeled for this specific sensor are (interior calibration):
 - Vertical and horizontal rotation correction (δ_i, β_i)
 - Vertical and horizontal offset (H_0^i, V_0^i)
 - Distance offset (D_0^i)
 - Distance scale factor (s_i)



Previous work

- **Previous analysis (Lichti & Glennie) have performed a planar feature based least-square adjustment to find the internal calibration parameters**
 - The performance of individual lasers is not uniform.
 - Temporal instability (VLP-16): stability of measurements during long-term recordings
 - Temperature instability (HDL-64E): effect of temperature variations and time needed to get into a steady state
- **They demonstrated that their sensor fulfills the manufacturer's stated accuracy of its specifications**
 - To take in to account that the data is collected at short ranges to the target
 - It is highlighted that some laser channels behave significantly poorer than others
- **Therefore, the present work shows the methodology we used to evaluate the performance of each laser channel and characterize them independently of each other.**
- **Moreover, we evaluate the measurements of the sensor in a wider span of ranges**
 - From 1 m up to 20 m

Calibration setup



- **Manufacturer specifications for the VLP-16 Puck**

Sensor	16 lasers
	FOV-V: 30° (+15° to -15°)
	FOV-H: 360 °
	3 cm accuracy
Laser	Class 1
	903 nm wavelength
	3.0 mrad horizontal beam divergence
	1.5 mrad vertical beam divergence

- **Configuration used during measurements**

Rotation rate	10 Hz
Return mode	Strongest
Phase Lock	off

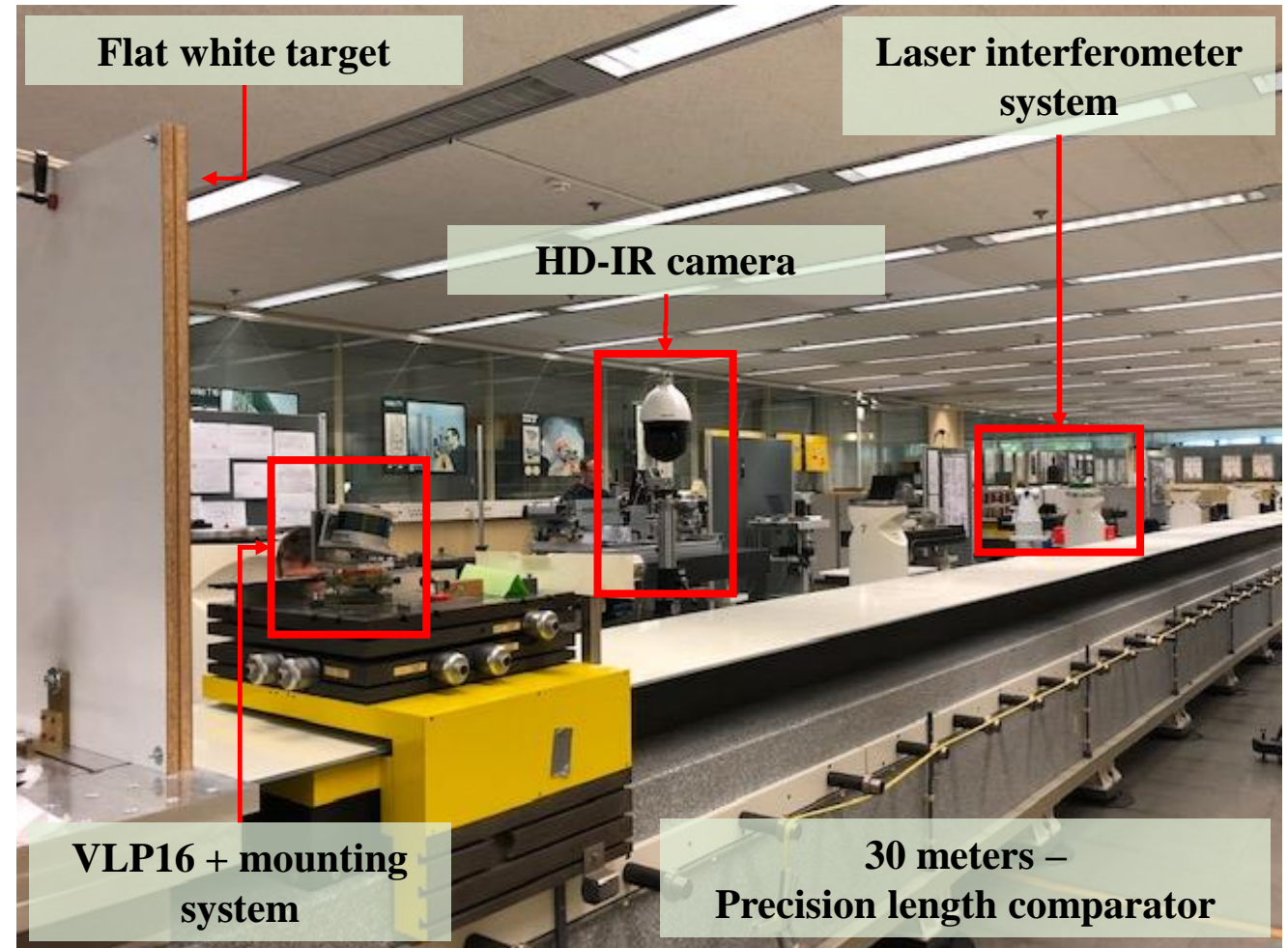
Calibration setup



Measurements at:

1 m, 2 m, 4 m, 6 m, 8 m

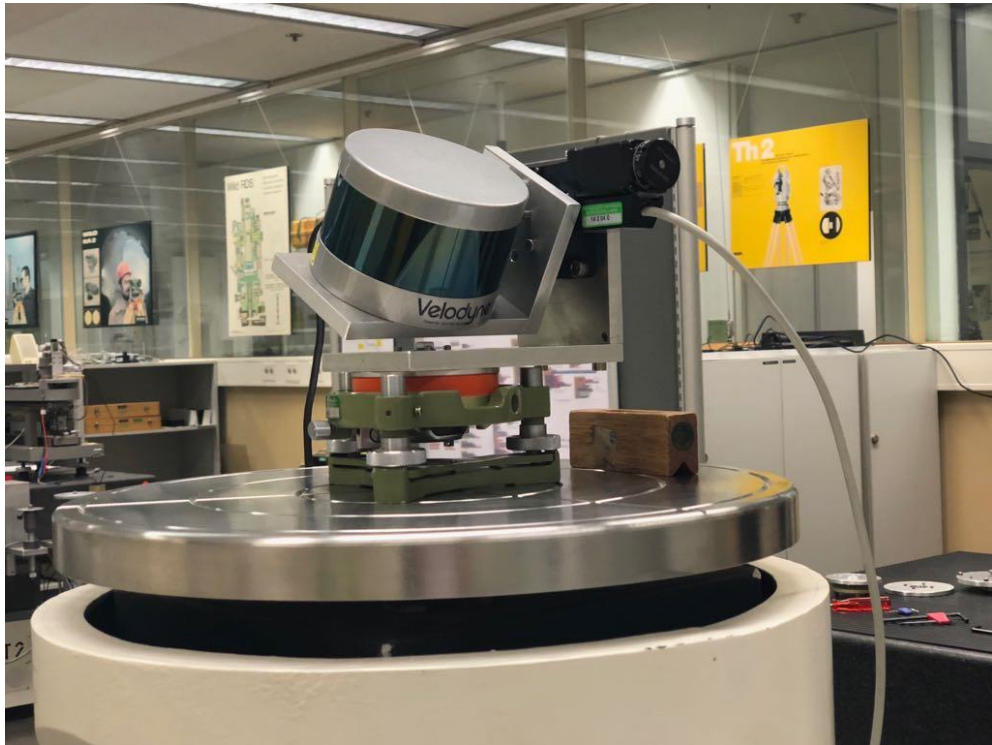
10 m, 12.5 m, 15 m, 17.5 m, 20 m



Calibration setup



VLP-16 mounting



- To steer electronically the laser channels of the sensor and thus, have control of the direction in which the lasers intersect the surface of the target
- A rotation is applied around the x-axis of the sensor
- Maximum accuracy of the applied rotation is 1/20 of a degree
- Approximately the duration of each recording is 20s
- Before the measurements 30 minutes to warm up the sensor and get to a steady state
- The sensor was never powered off during the measurements

Calibration setup



HD-IR camera [left]

- Used to visualize the lasers on the surface of the target and apply the correct pitch to align the laser to the xy-reference plane of the sensor

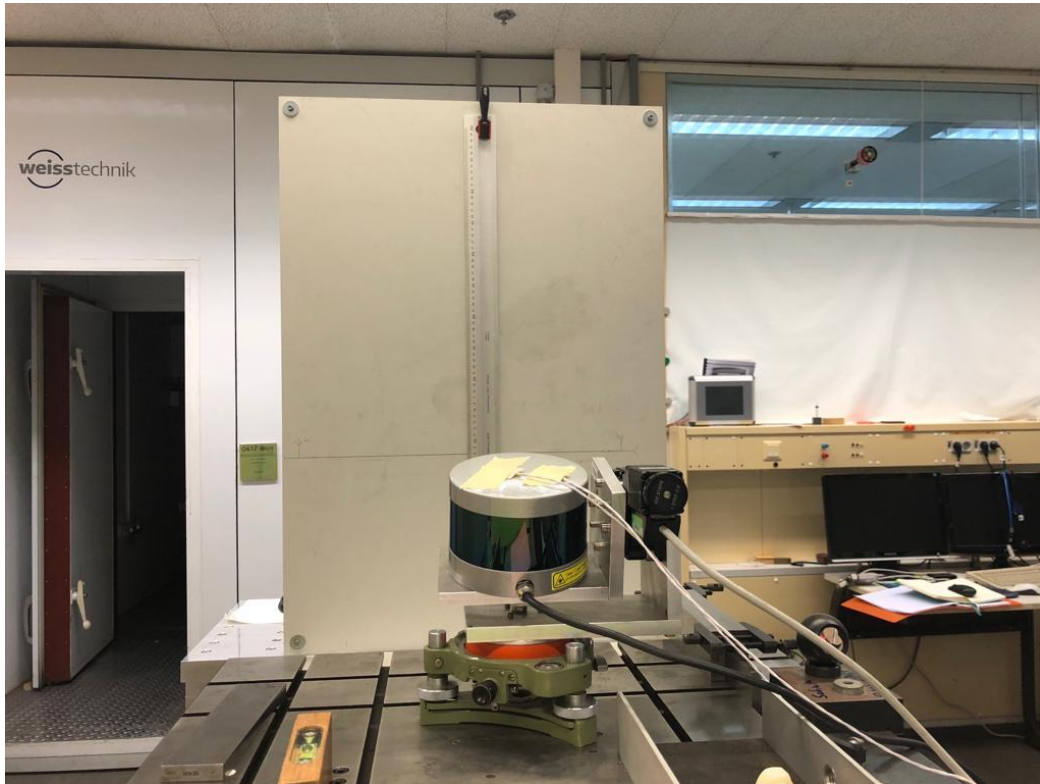
Laser interferometer [right]

- Used to place the sensor at a specific distance from the target
- It has an automatic line of capture with an uncertainty of $0.6 \mu\text{m}$

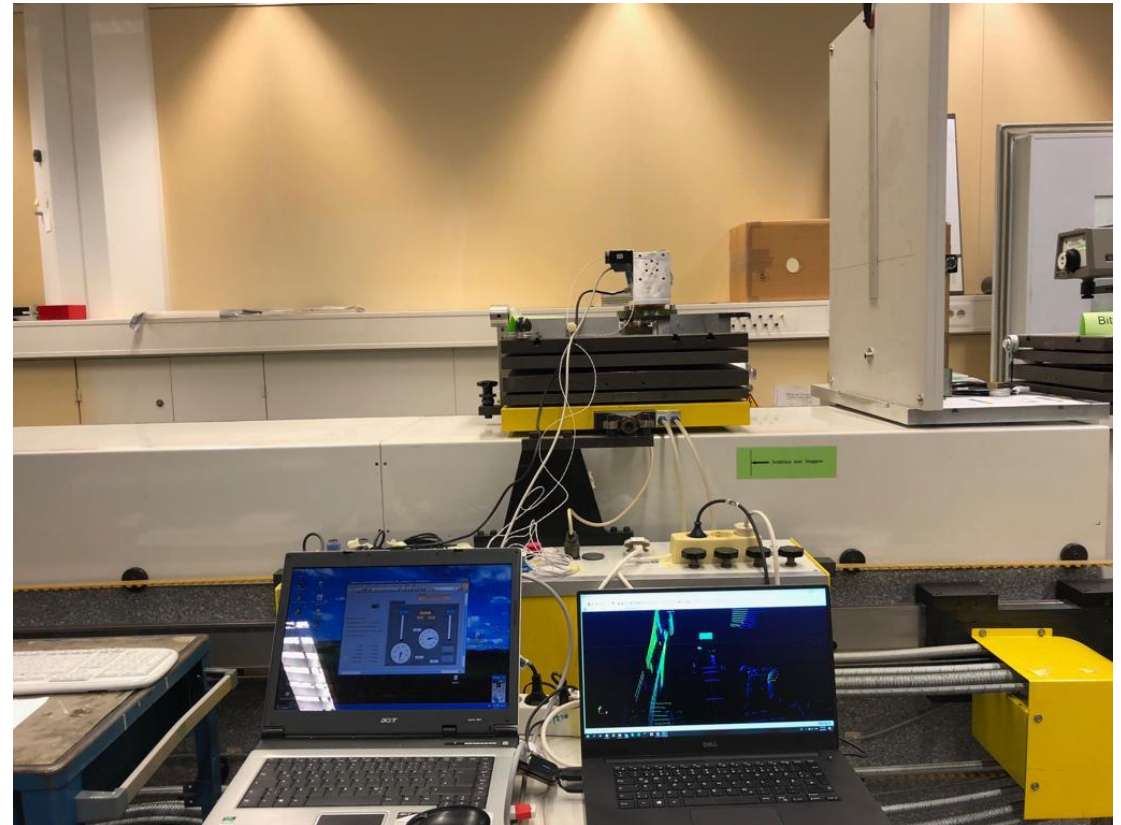


Calibration setup

IV



Front view (sensor's perspective)



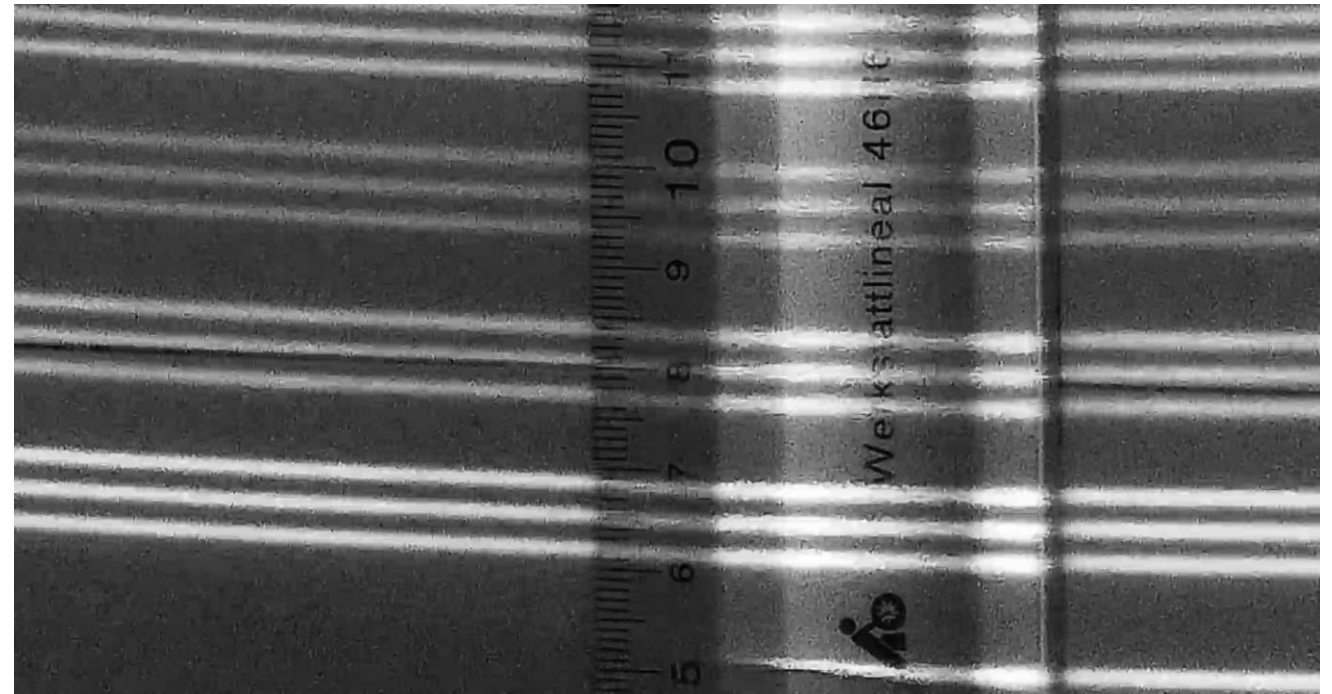
Lateral view

Calibration setup

V

Sample picture from the HD-IR camera

- Each triad comes from each of the 16 lasers that are integrated in the sensor.
- For each triad, the one in the middle was taken as reference to align the lasers to x-y reference plane.
- To choose the right pitch to apply to each laser, measurements were done at: 0.75m, 1m, 2m.

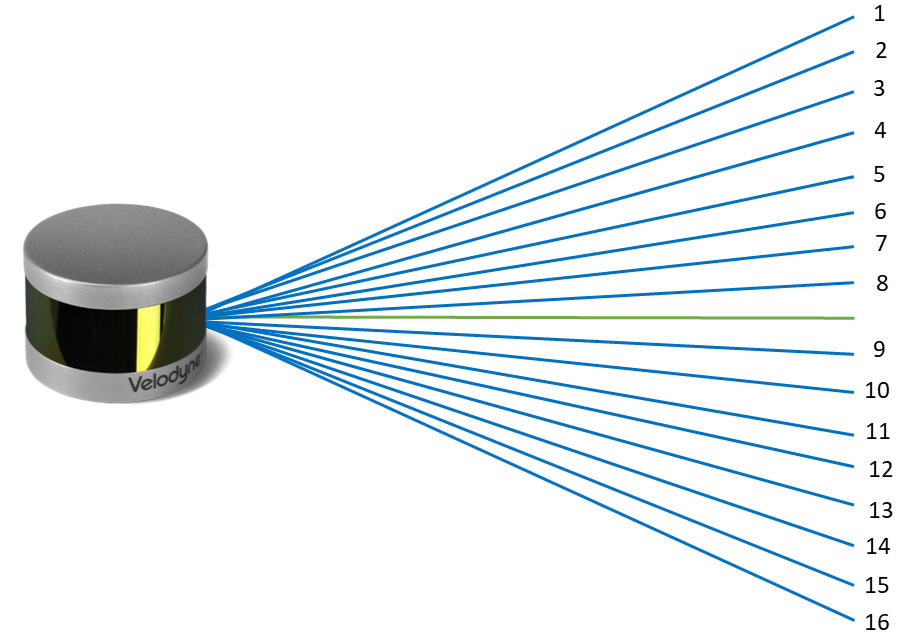


Laser spot pattern (Stacked laser diodes)

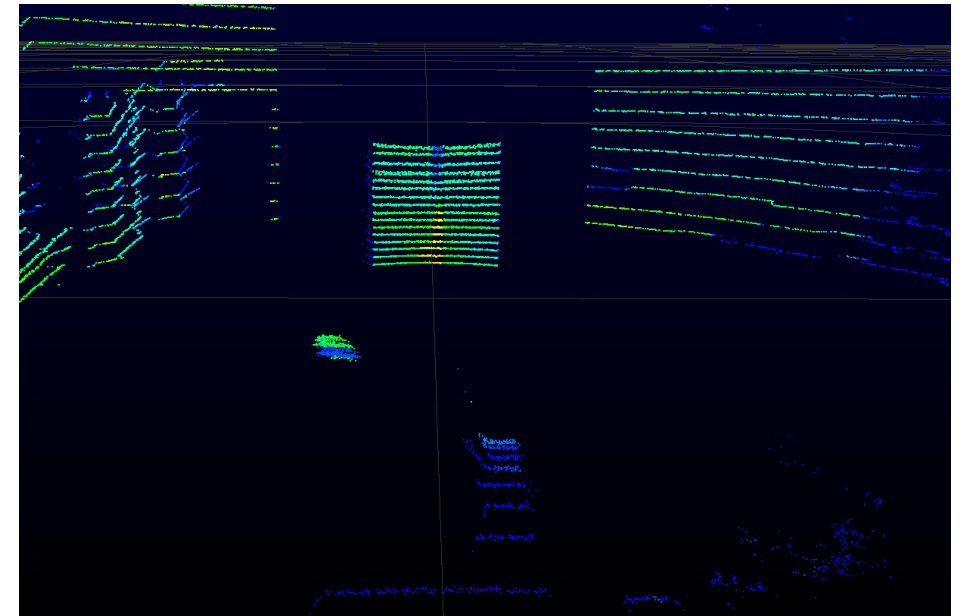
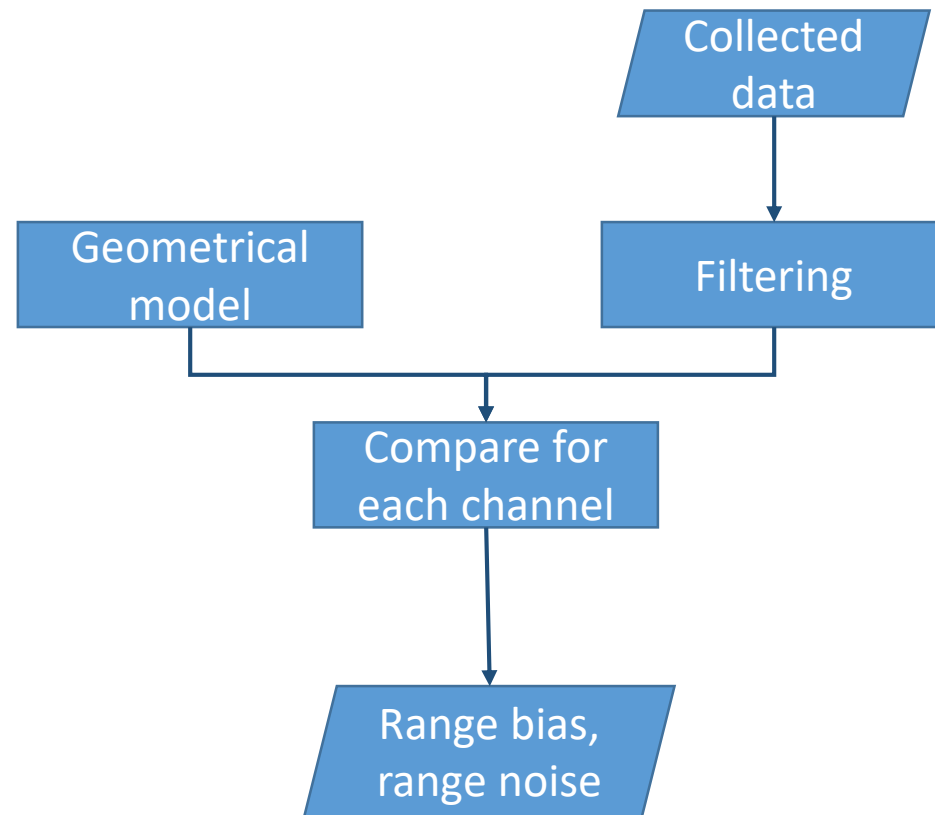
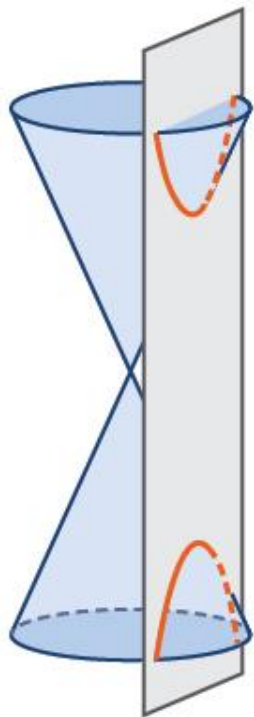
Calibration setup

VI

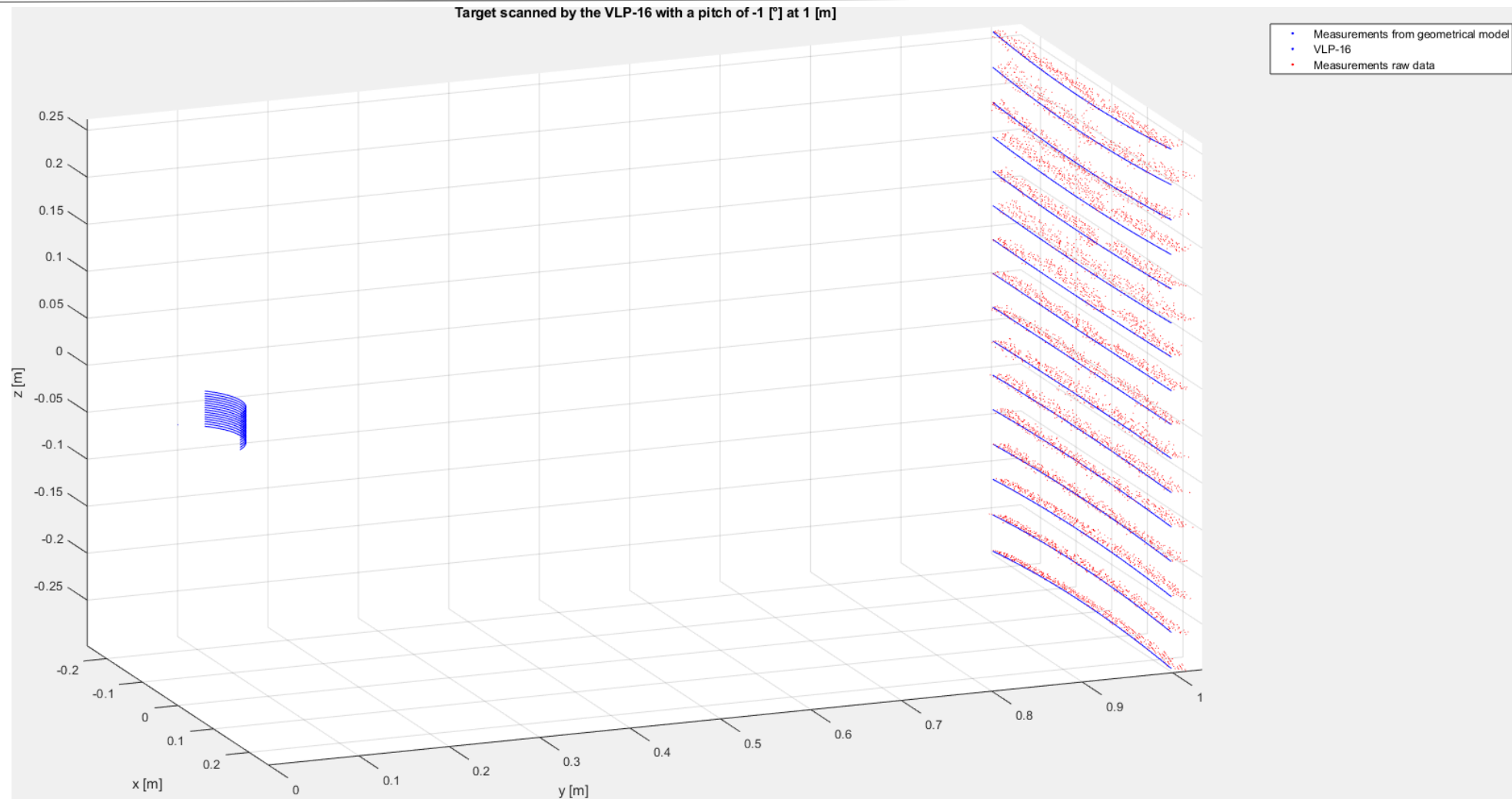
Channel	Theoretical El [deg]	El @ 0.75m [deg]	El @ 1m [deg]	El @ 2m [deg]	Hz resolution [deg]	Symmetry
1	15	14.71	14.35	14.70		
2	13	12.30	12.45	12.75	1.95	
3	11	10.40	10.55	10.80	1.95	
4	9	8.50	8.65	8.85	1.95	
5	7	6.40	6.55	6.75	2.10	
6	5	4.50	4.65	4.85	1.90	
7	3	2.80	2.85	2.95	1.90	
8	1	0.80	0.85	0.95	2.00	
9	-1	-1.00	-1.05	-1.00	1.95	
10	-3	-2.90	-2.95	-2.95	1.95	
11	-5	-4.90	-4.95	-4.95	2.00	
12	-7	-6.70	-6.80	-6.90	1.95	
13	-9	-8.55	-8.75	-8.85	1.95	
14	-11	-10.45	-10.65	-10.80	1.95	
15	-13	-12.45	-12.65	-12.80	2.00	
16	-15	-14.25	-14.45	-14.70	1.90	



Data Processing

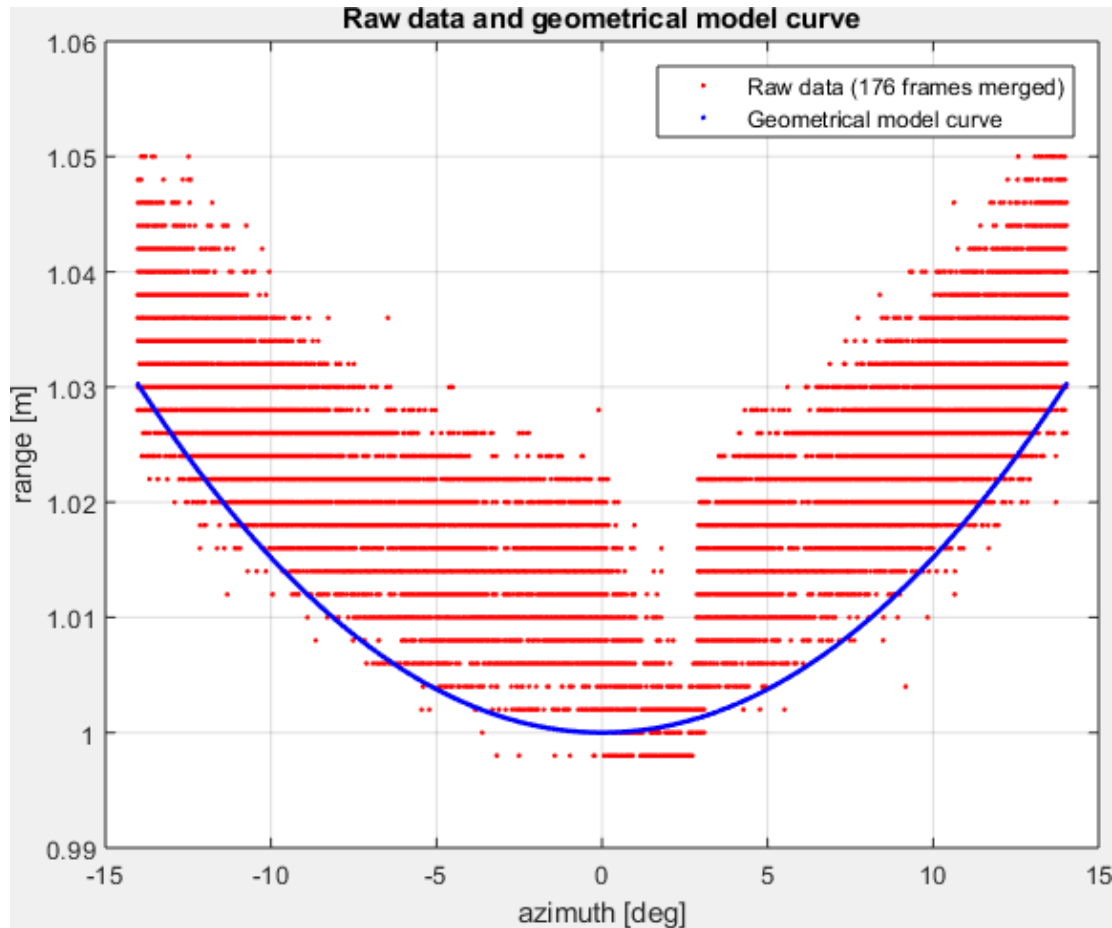


Data Processing

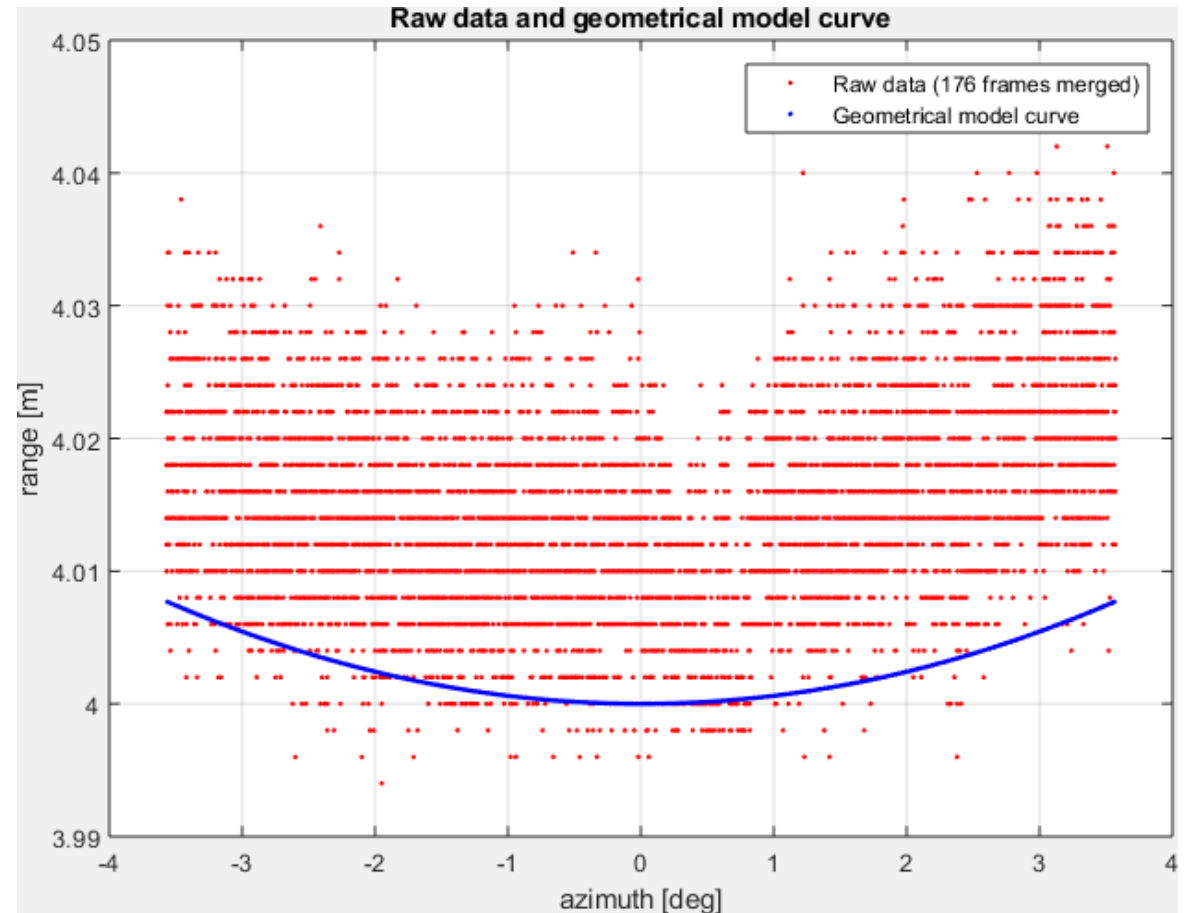


Preliminary results

Channel 5 at 1m



Channel 6 at 4m

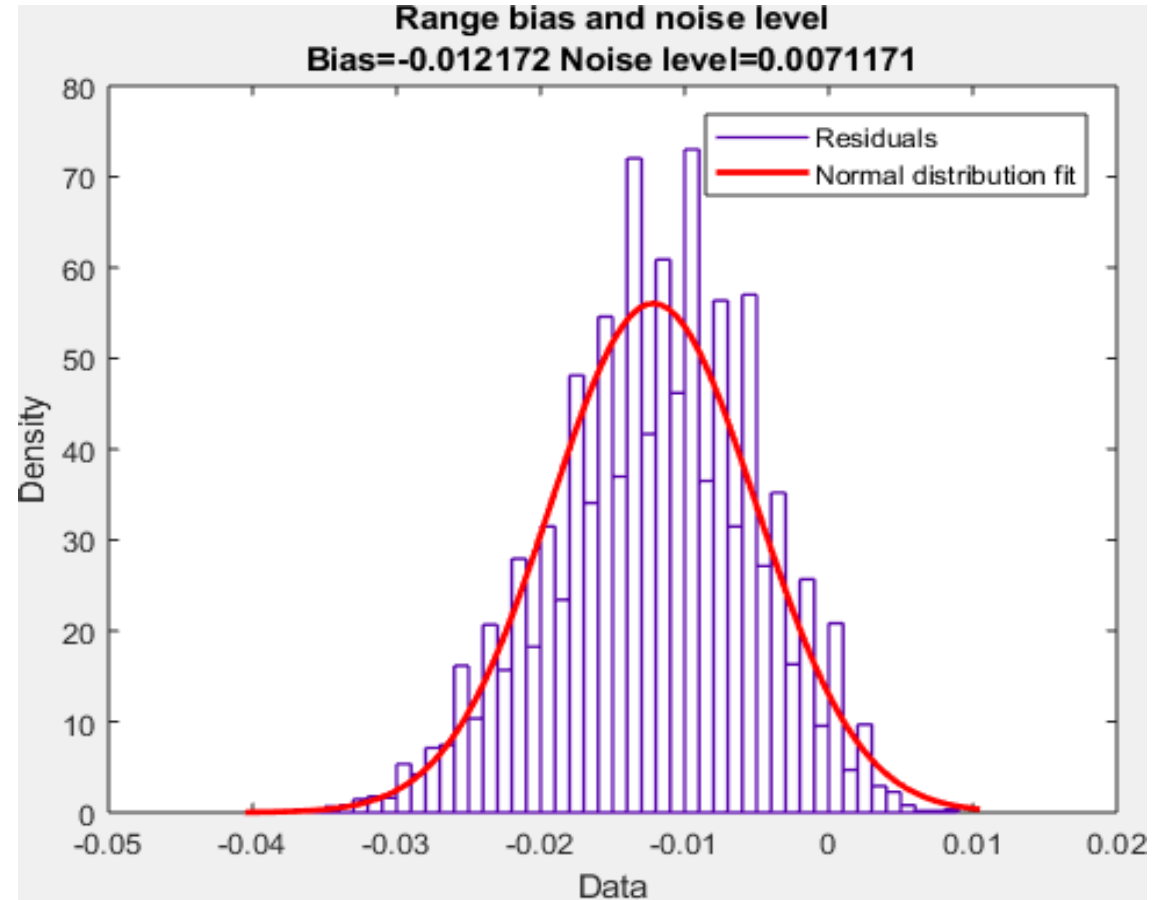
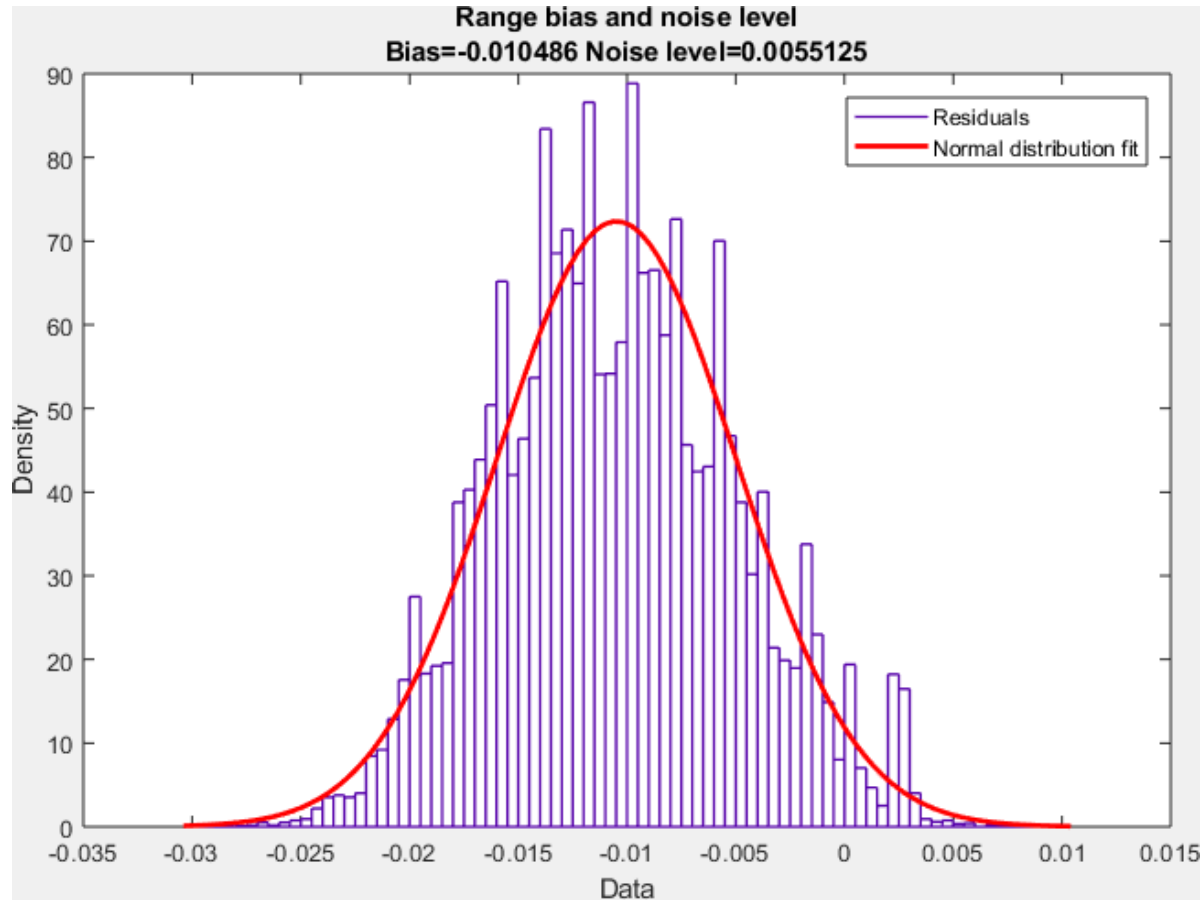


Preliminary results



Channel 5 at 1m

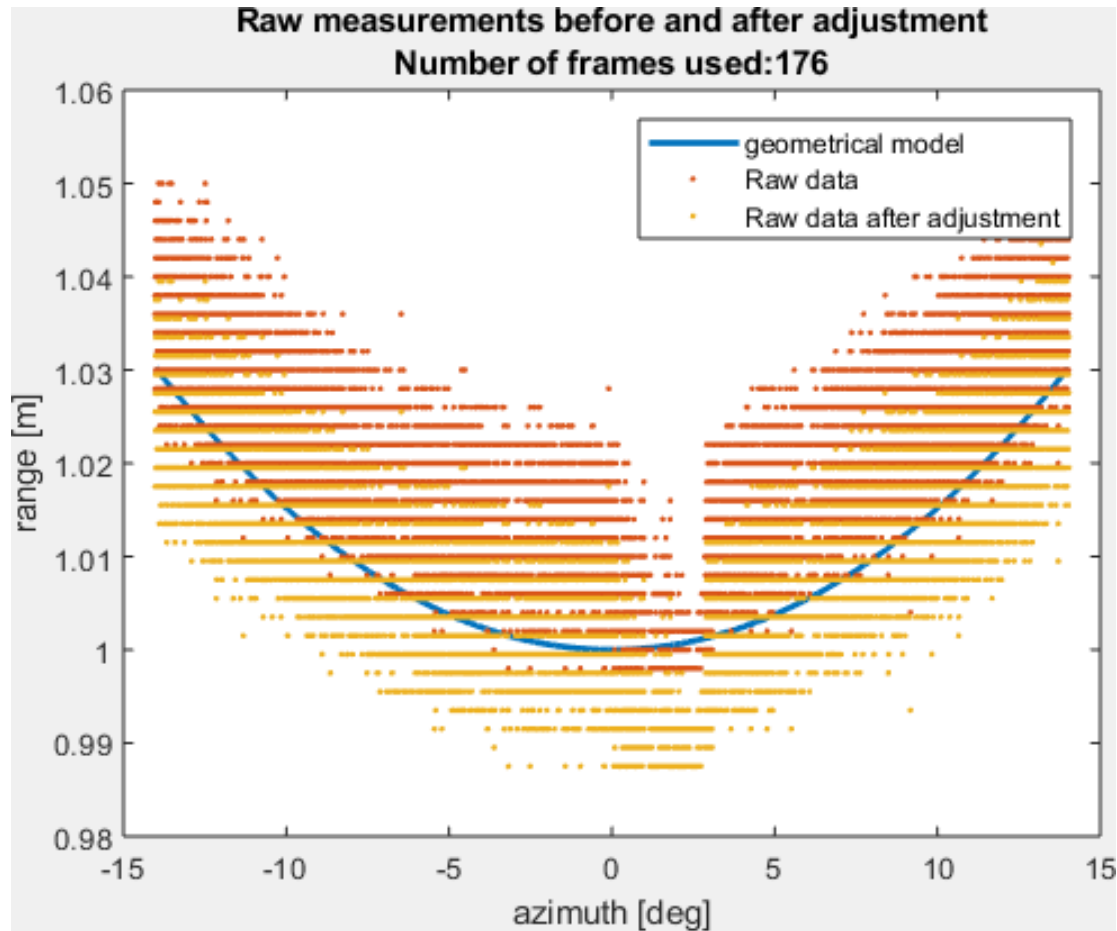
Channel 6 at 4m



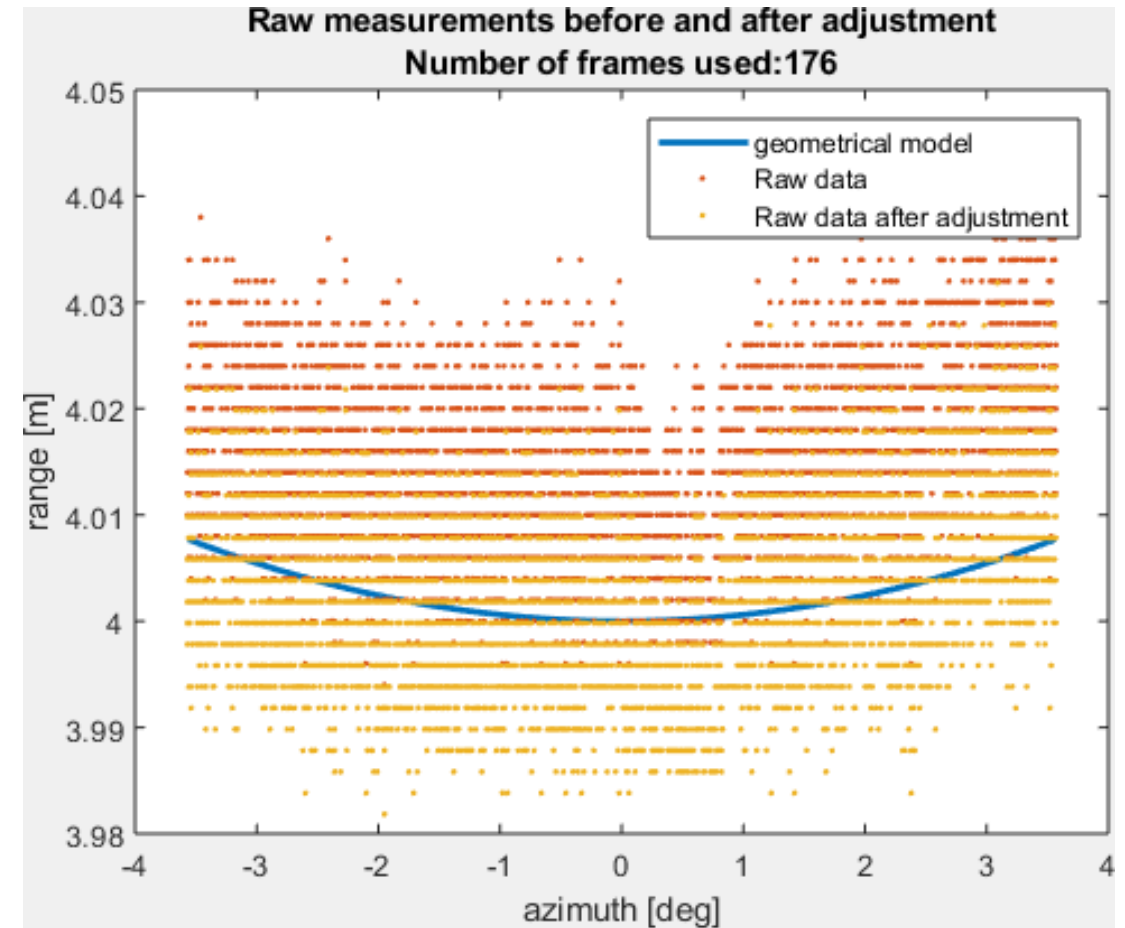
Preliminary results



Channel 5 at 1m



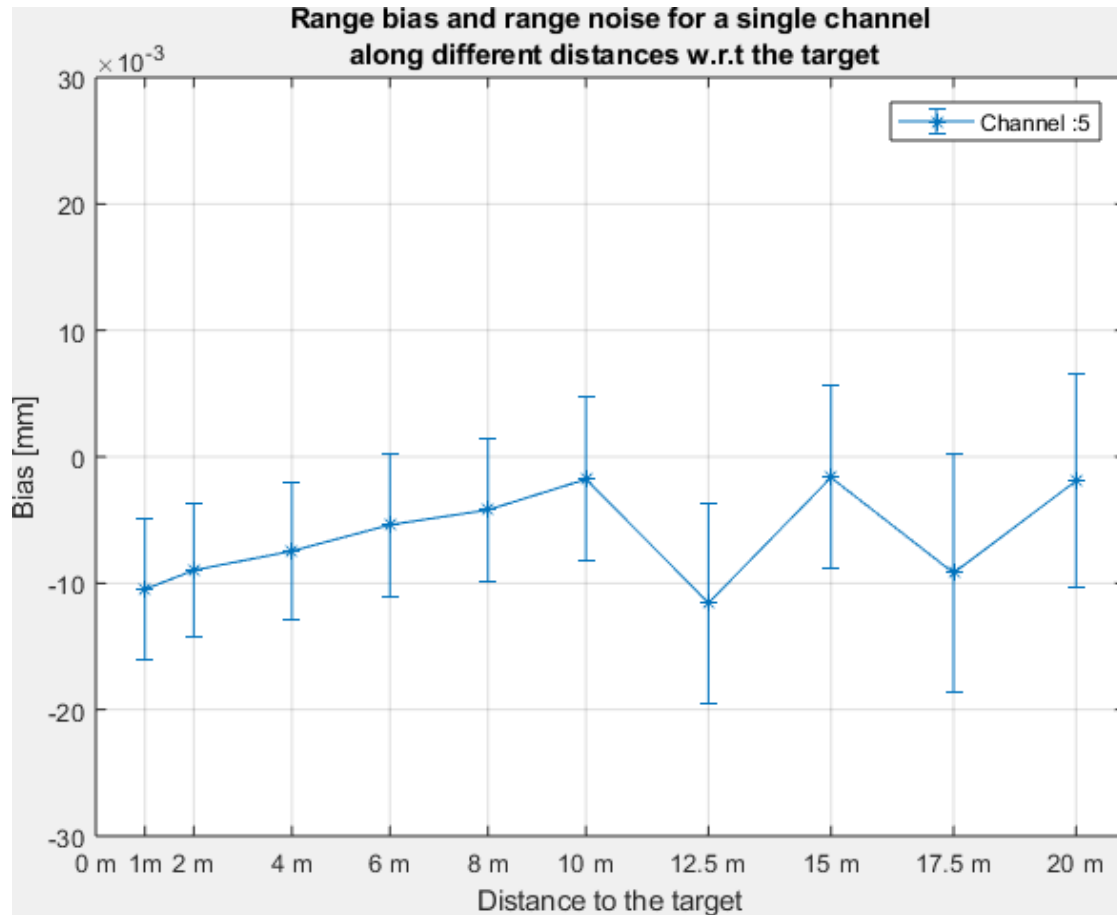
Channel 6 at 4m



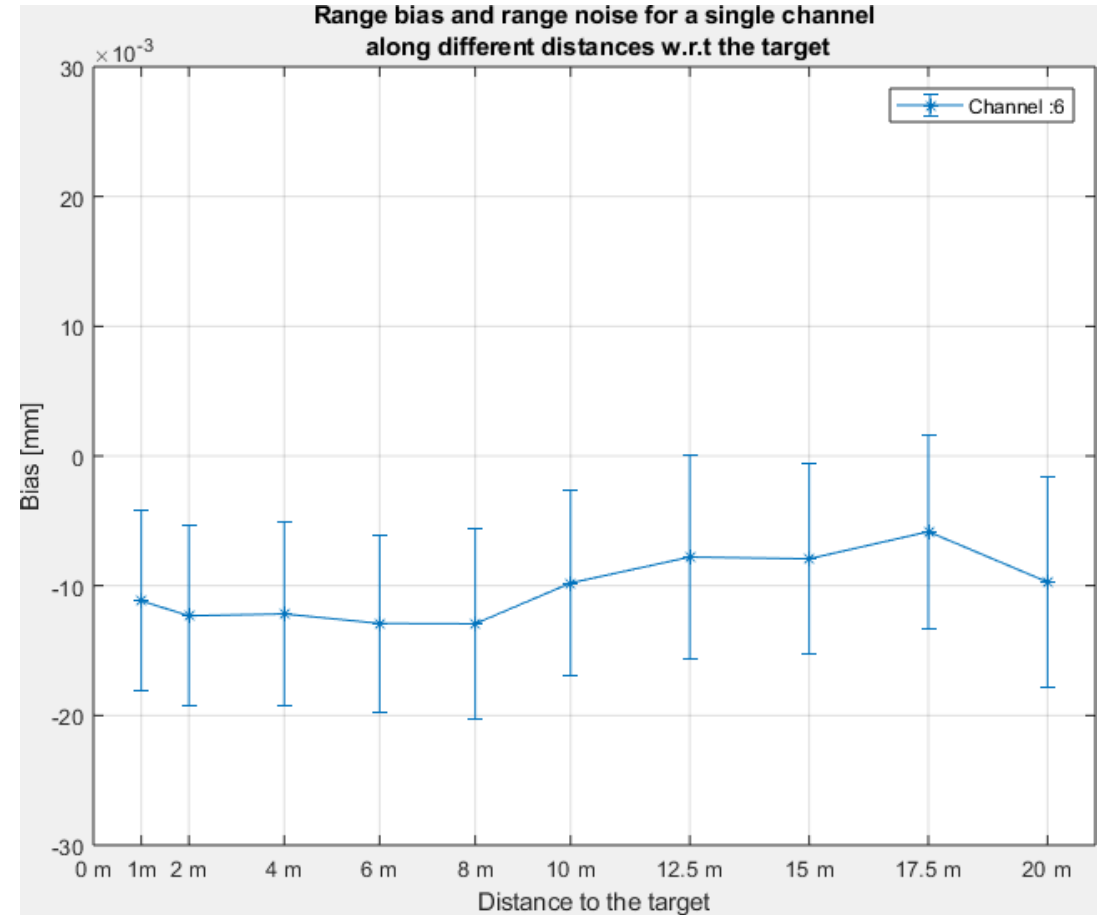
Preliminary results

IV

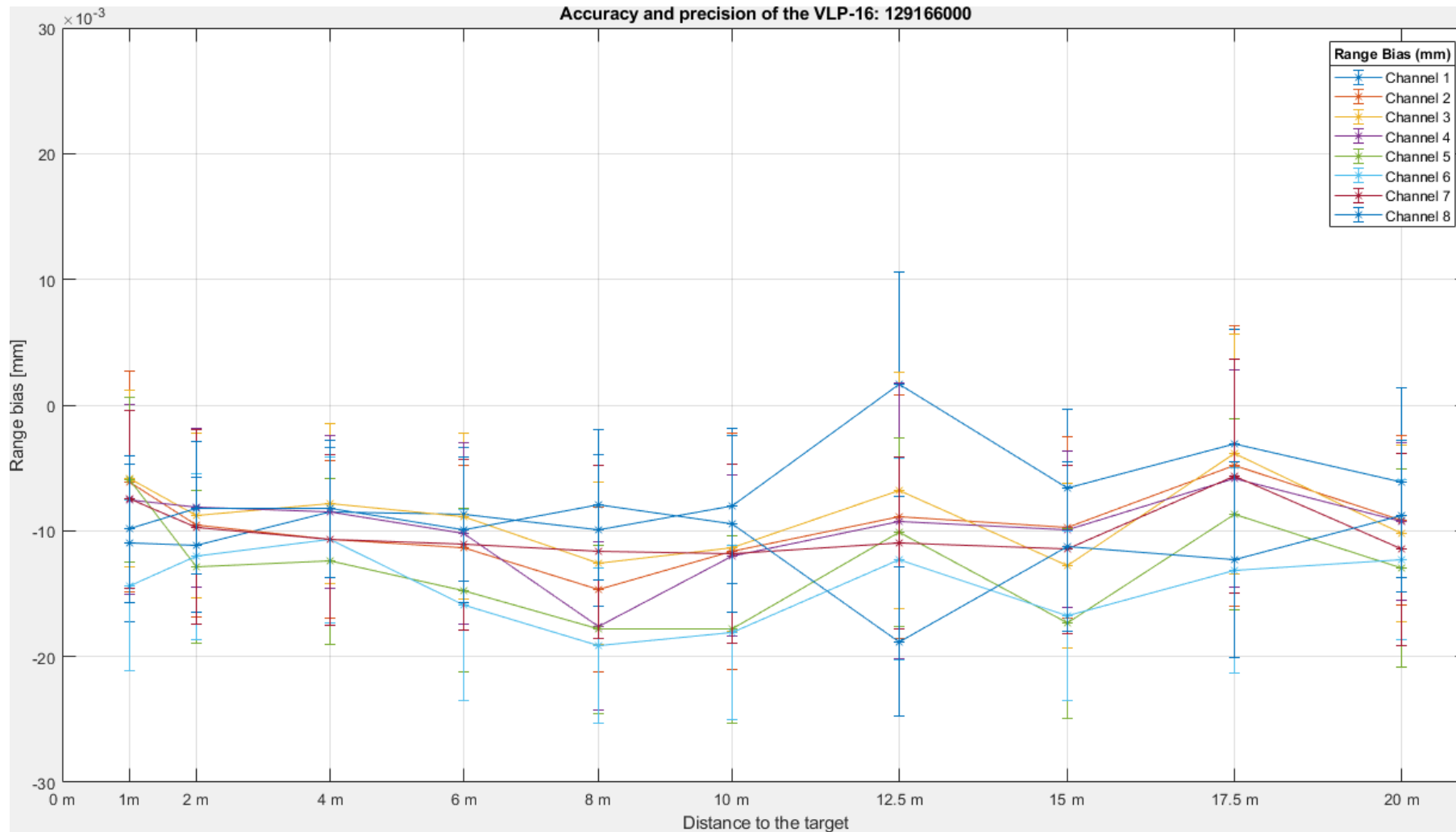
Channel 5



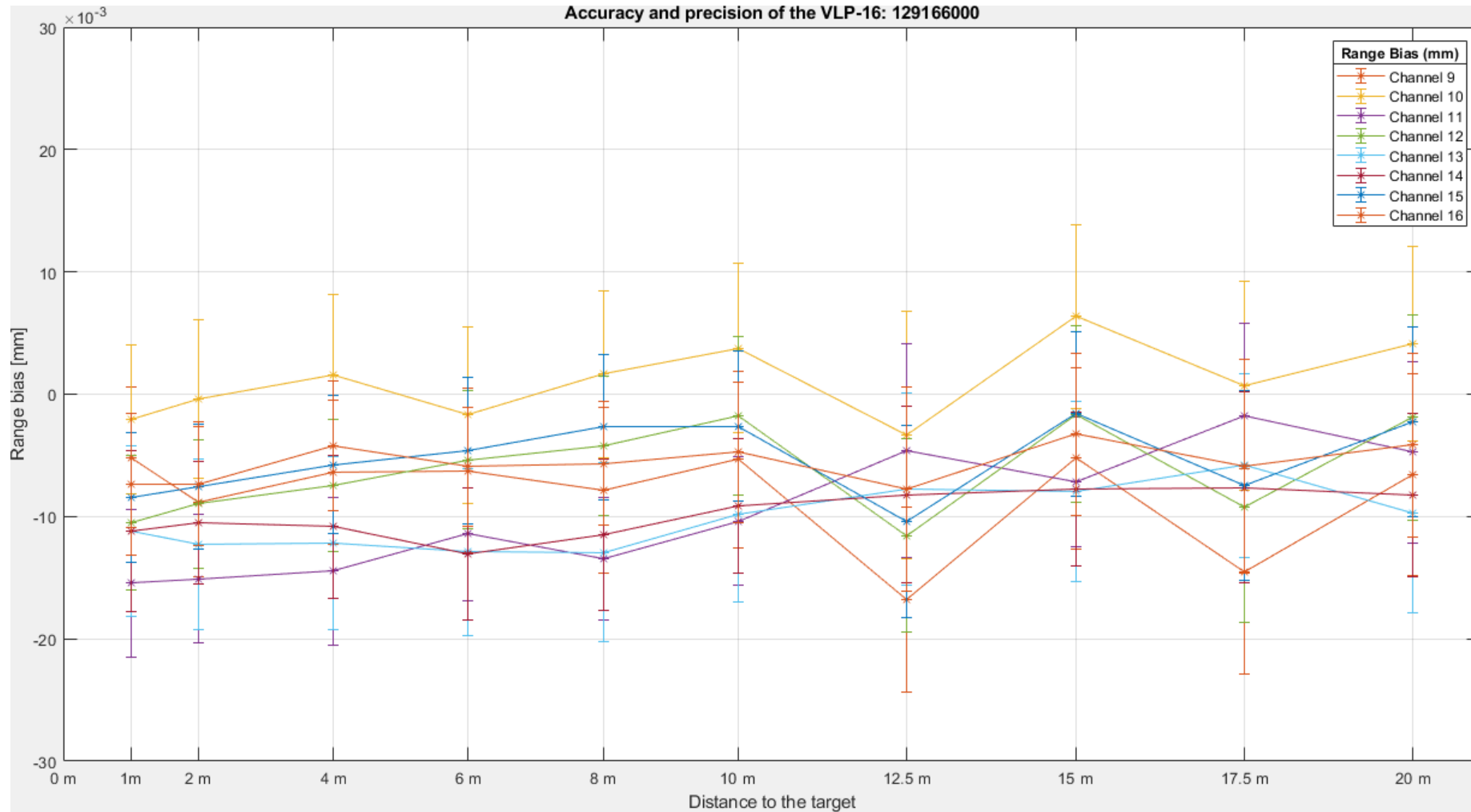
Channel 6



Results



Results



Conclusions

- **Fulfills the specifications of the sensor**
- **Agrees with previous work done by Lichti and Glennie**
 - Range noise vary from 5-12 mm
 - Maximum range bias of 20 mm
- **Contrary to Lichti, the lasers that were looking more downward were not performing worse than the others.**
- **A correction can be applied to enhance the accuracy of the measurements, although it not may be significant for automotive applications**
- **The biggest disadvantage is the noise in the data (due to the mechanical moving parts)**
- **To inquire:**
 - Relationship between reflection properties of targets and range measurements



Contact

Daniela E. Sánchez Morales

Institute of Space Technology and Space Applications

Universität der Bundeswehr München

Email: daniela.sanchez@unibw.de

Phone: +49 (0)89 6004 2584

Supported by:

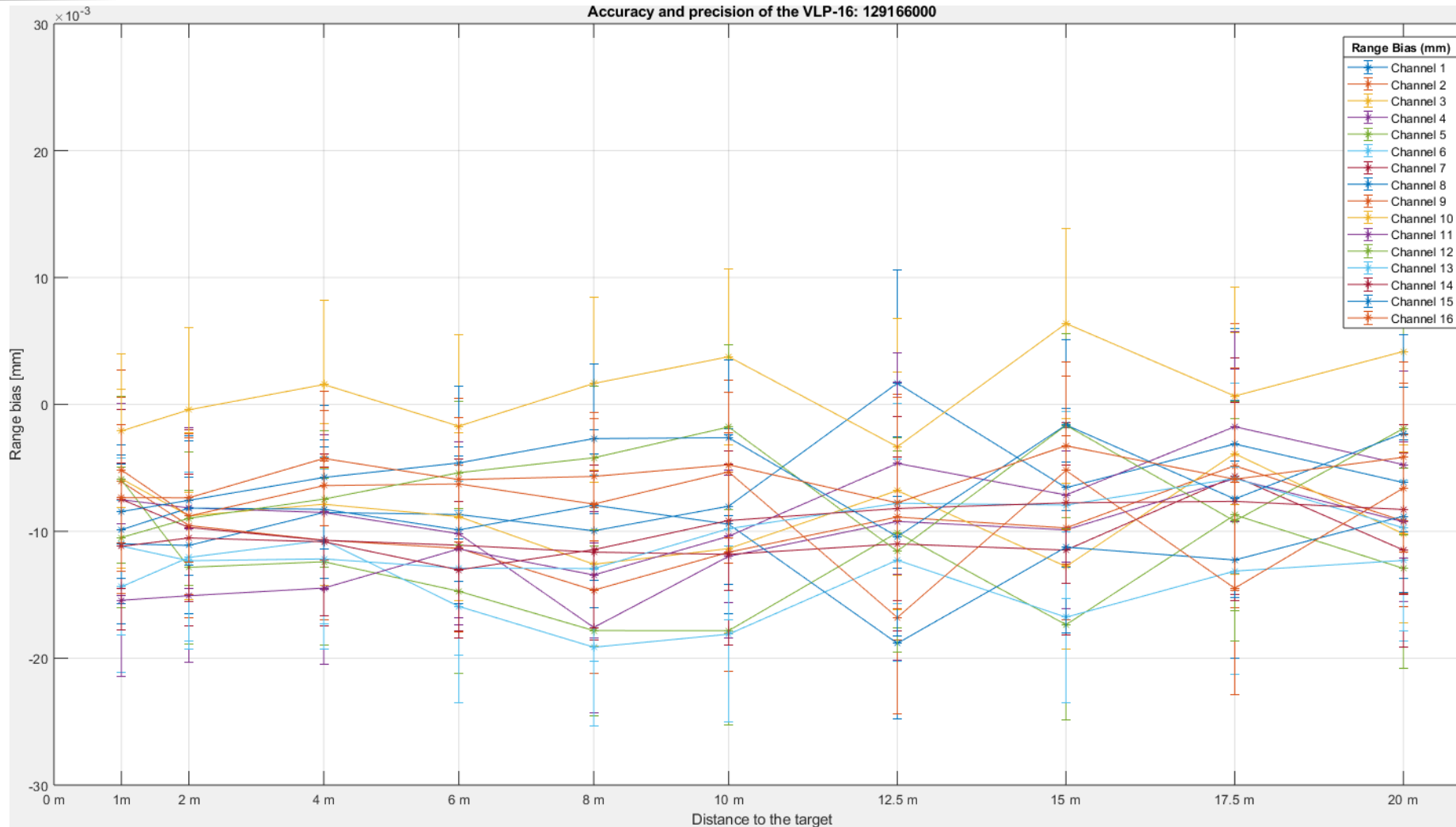


Federal Ministry
for Economic Affairs
and Energy

on the basis of a decision
by the German Bundestag

Additional material

Results



Other systematic errors (artifacts)

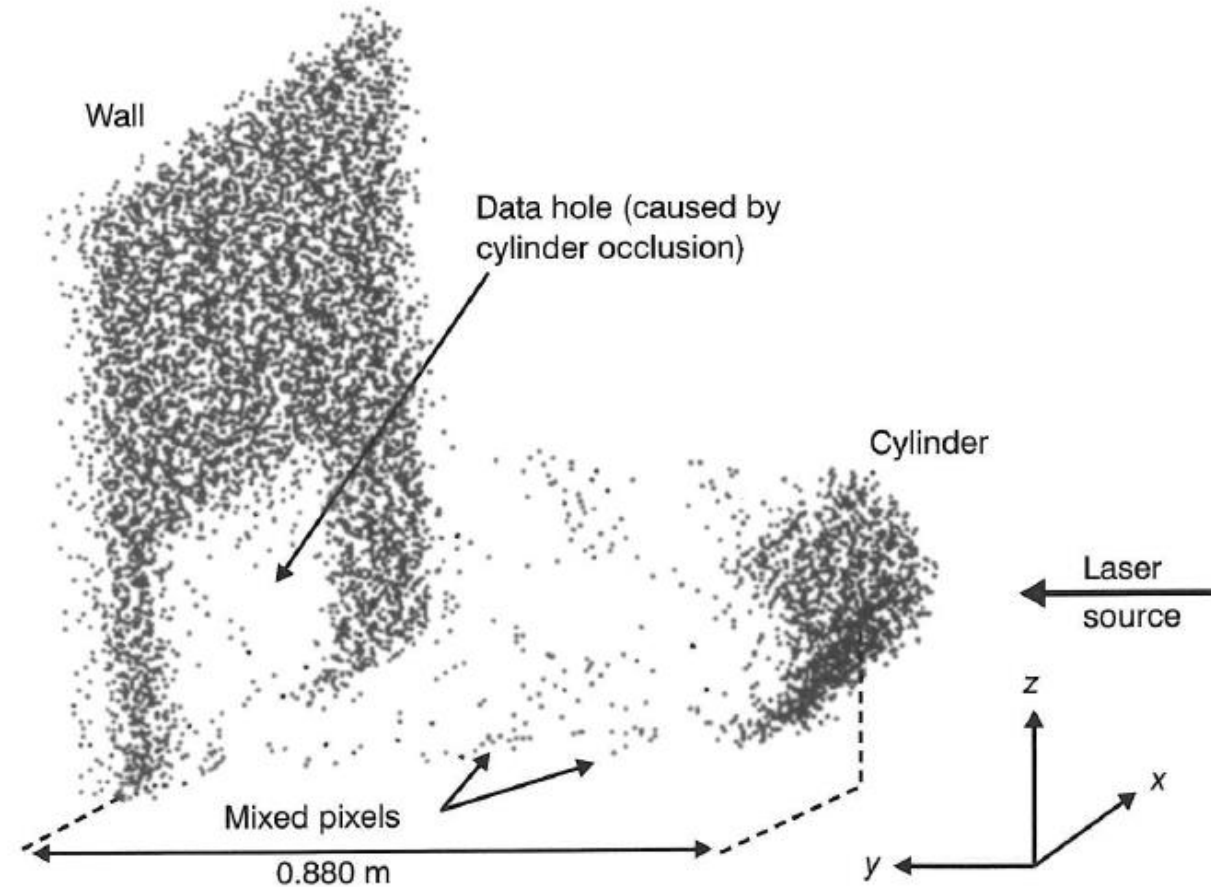


Figure . Subsystem error contribution (without GPS) to target error for a terrestrial vehicle system (LMS-Q240). (Imagen taken from Glennie,2007)

Other systematic errors (artifacts)

II

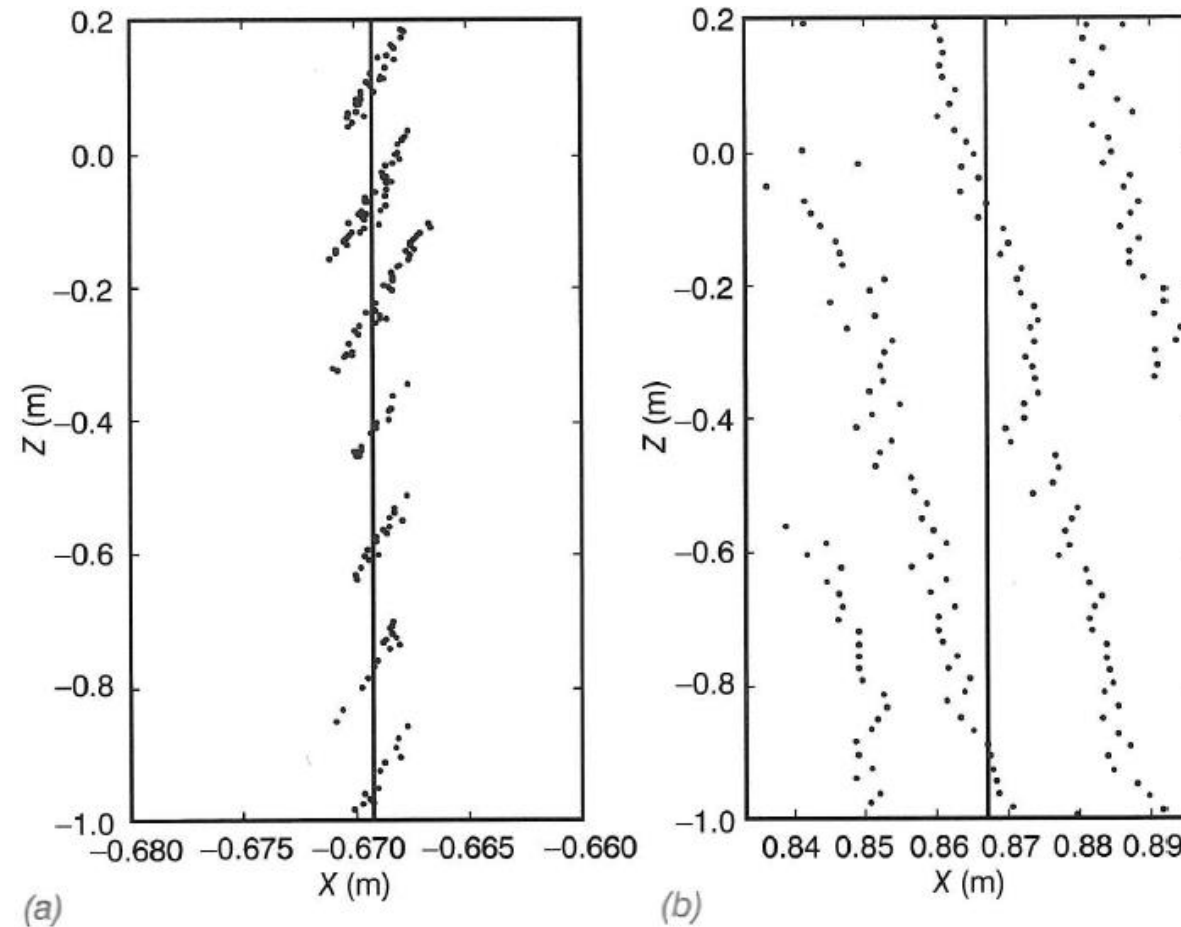


Figure . Subsystem error contribution (without GPS) to target error for a terrestrial vehicle system (LMS-Q240). (Imagen taken from Glennie,2007)

Other systematic errors (artifacts)

III

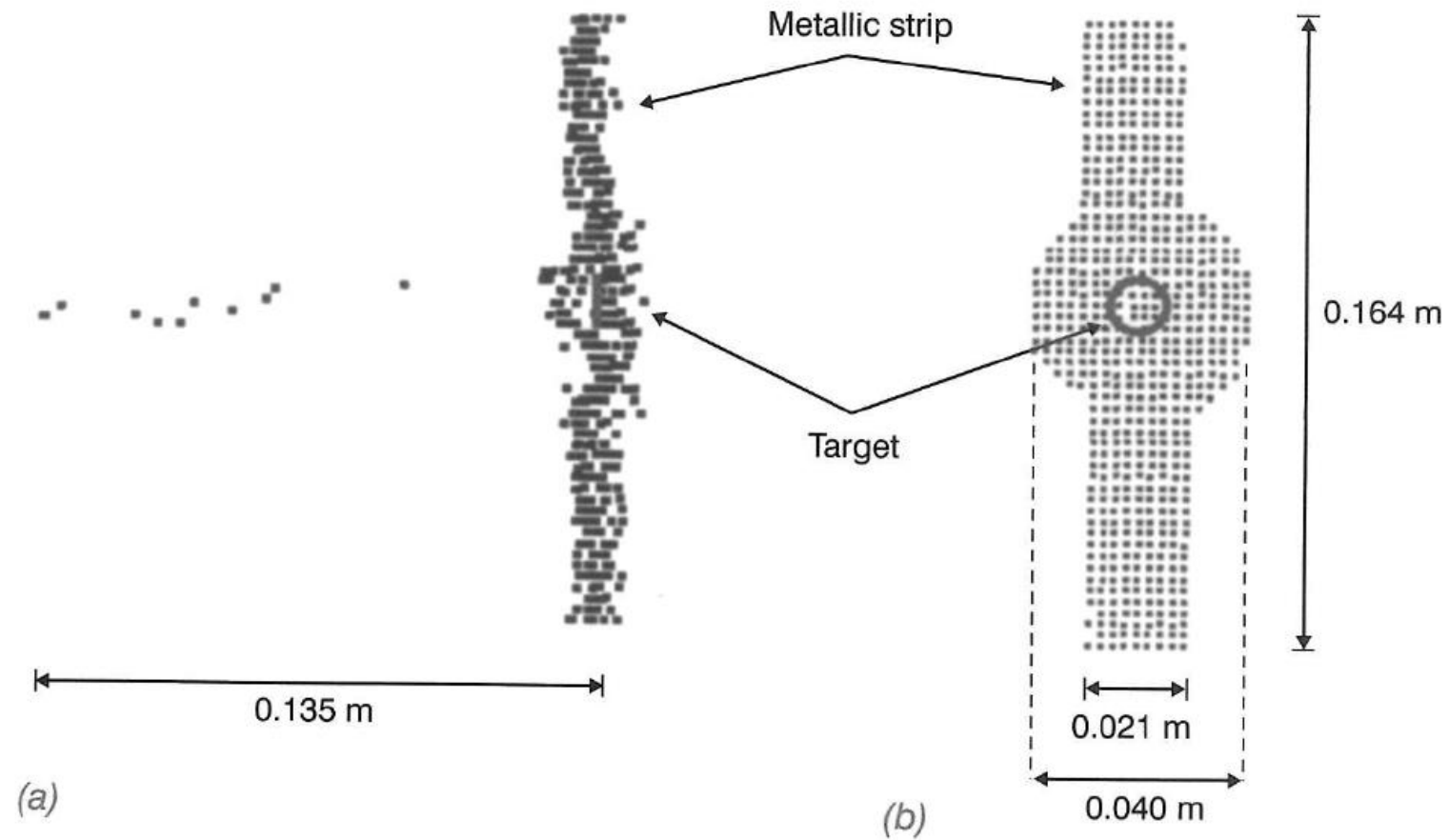
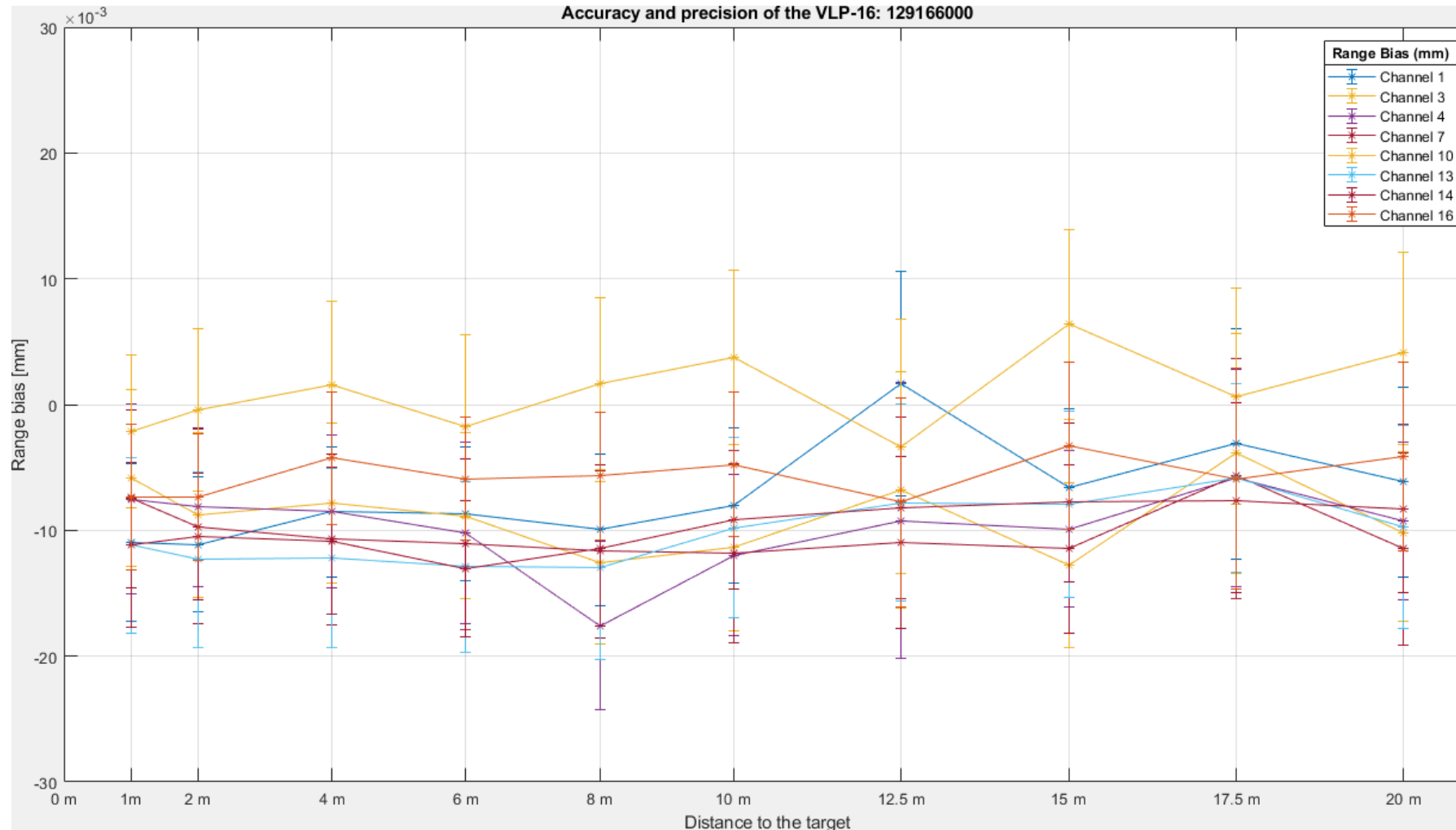
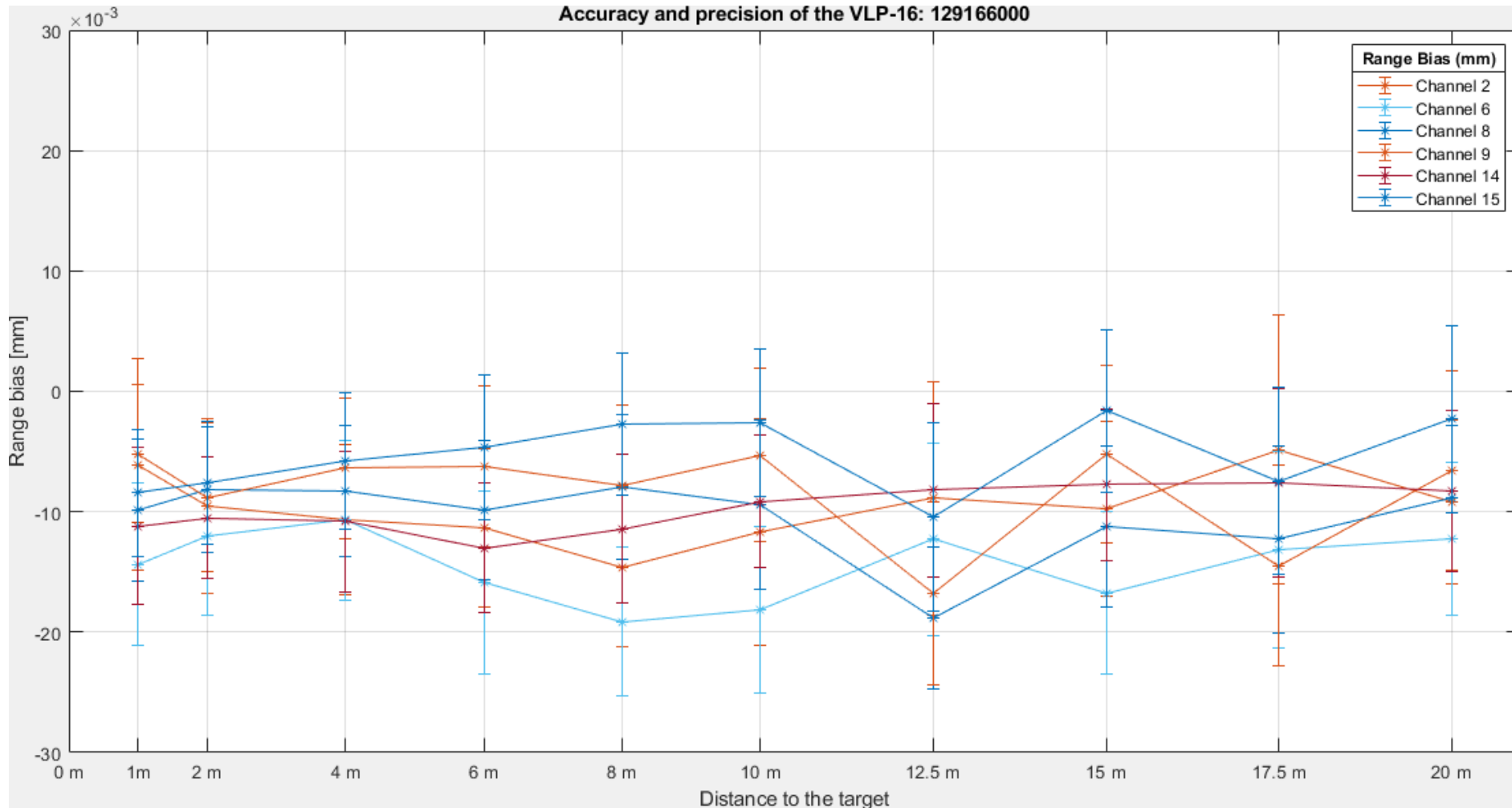


Figure . Subsystem error contribution (without GPS) to target error for a terrestrial vehicle system (LMS-Q240). (Imagen taken from Glennie,2007)

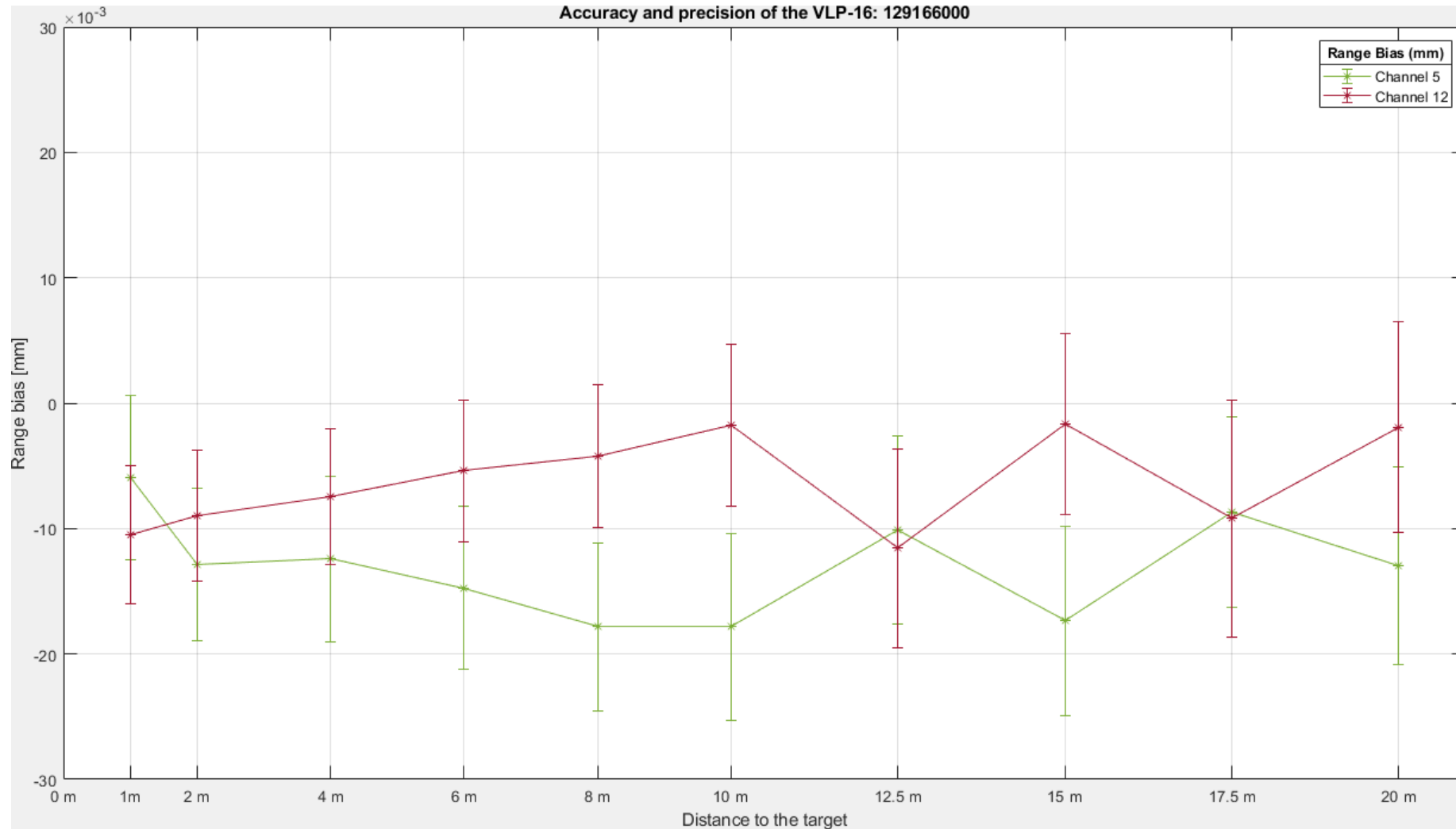
Range bias and noise (g)



Range bias and noise (o)



Range bias and noise (r)



Target accuracy error budget

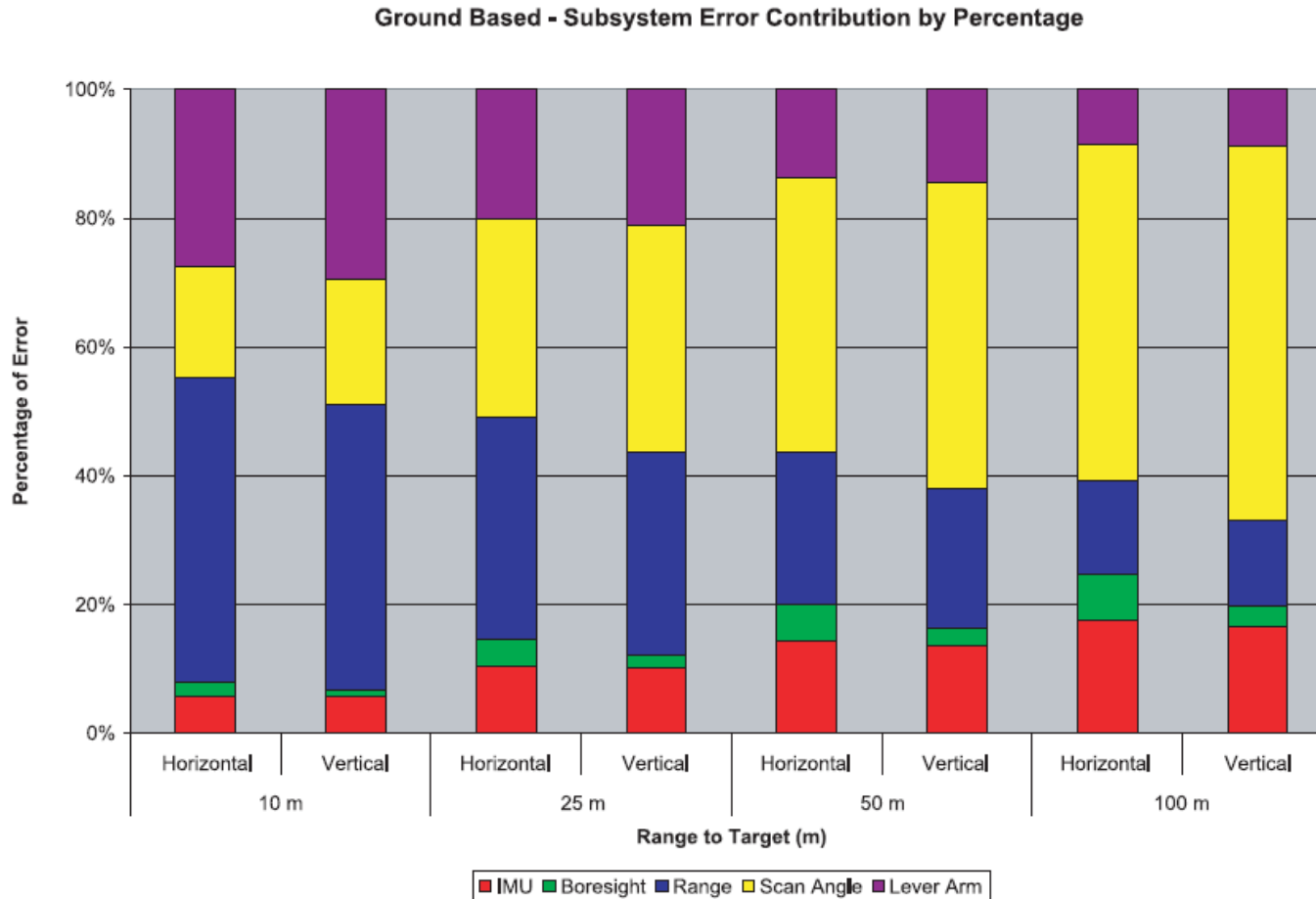


Figure . Subsystem error contribution (without GPS) to target error for a terrestrial vehicle system (LMS-Q240). (Imagen taken from Glennie,2007)

Other systematic errors (artifacts)

$$\Delta\rho = A_0 + A_1\rho + A_2 \sin \alpha + \sum_{k+1}^n \left(A_{2k+1} \sin \left(\frac{2\pi k\rho}{U_1} \right) + A_{2k+2} \cos \left(\frac{2\pi k\rho}{U_1} \right) \right) + ET$$

Additive constant

Scale error

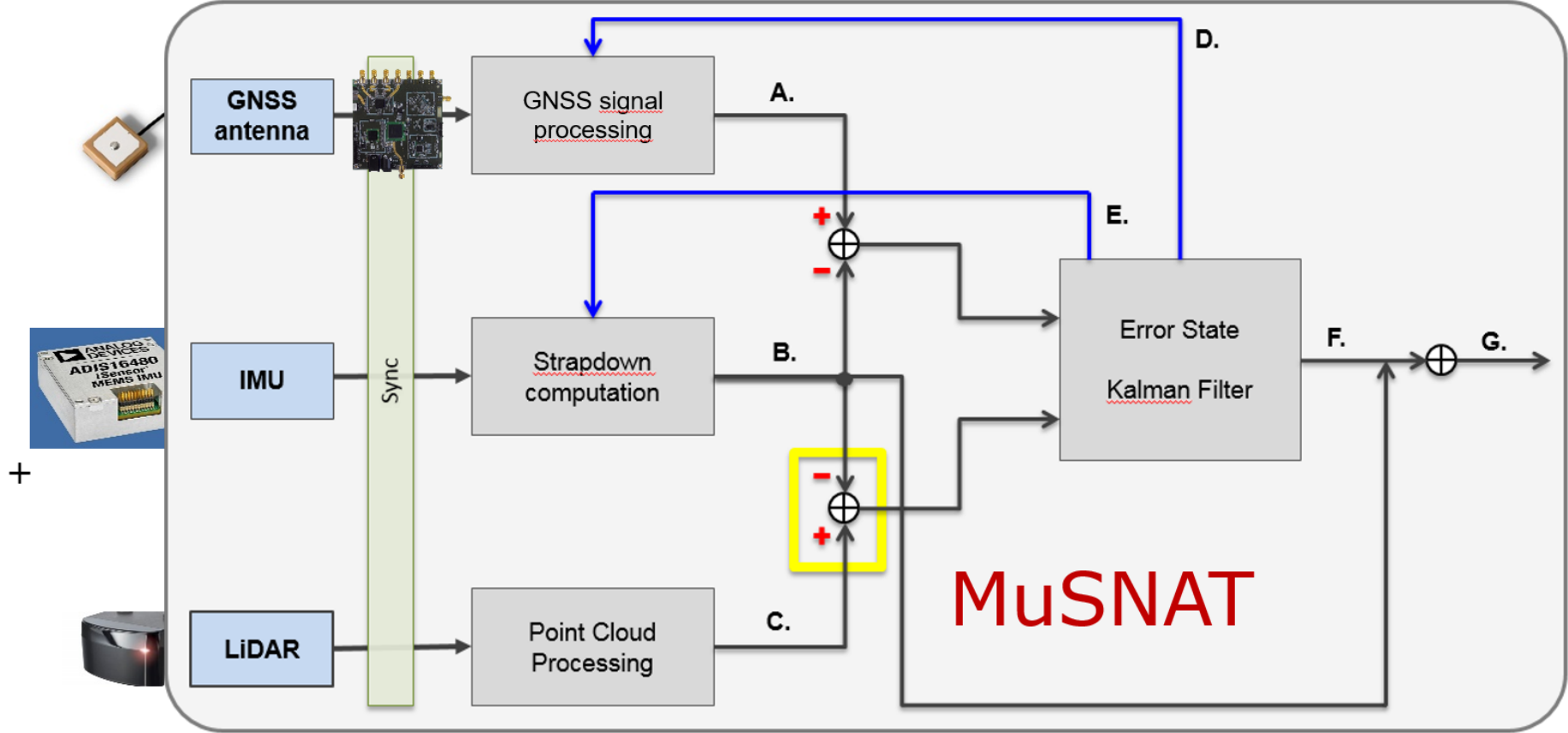
Vertical offset of the laser axis from the trunnion axis

Cyclic error terms caused by internal optical or electrical interference*

Empirical terms

* Only relevant for rangefinders that operate using the phase-difference measurement principle

Deep Sensor Fusion (GNSS, INS and LiDAR)



A. Position, code range, carrier and doppler; **B.** Position, velocity, attitude; **C.** Velocity, Dattitude; **D.** Feedback options: vector tracking, cycle slip corrections, synthetic aperture; **E.** Giro bias, acceleration

MuSNAT architecture

